

Electronic supporting information for

Modulating ICT emission: A new strategy to manipulate the CPL sign in chiral emitters

Josué Jiménez,^a Florencio Moreno,^a Beatriz L. Maroto,^a Trevor A. Cabreros,^b
Angelenia S. Huy,^b Gilles Muller,^b Jorge Bañuelos,^c and Santiago de la Moya^{*a}

^a *Departamento de Química Orgánica I, Facultad de Ciencias Químicas, Universidad Complutense de Madrid, Ciudad Universitaria s/n, 28040, Madrid, Spain. Fax: +34 91 394 4103; Tel: +34 91 394 5090; E-mail: santmoya@ucm.es*

^b *Department of Chemistry, San José State University, San José, CA 95192-0101, USA.*

^c *Departamento de Química Física, Facultad de Ciencias y Tecnología, Universidad del País Vasco-EHU, 48080, Bilbao, Spain.*

Table of contents

1.	General methods, instrumentation and techniques	S2
2.	Synthetic procedures and characterization data	S4
3.	¹ H and ¹³ C NMR spectra	S7
4.	Photophysical properties	S10
5.	References	S12

1. General methods, instrumentation and techniques

Anhydrous solvents were prepared by distillation over standard drying agents according to common methods. All other solvents were of HPLC grade and were used as provided. Starting chemical substrates and reagents were used as commercially provided unless otherwise indicated. Thin-layer chromatography (TLC) was performed with silica gel or alumina plates, and the chromatograms were visualized by using UV light ($\lambda = 254$ or 365 nm). Flash column chromatography was performed using silica gel (230-400 mesh) or on activated neutral alumina (activity degree 1, 70-290 mesh ASTM). Melting points are uncorrected. ^1H and ^{13}C NMR spectra were recorded in CDCl_3 solution at 20°C . NMR chemical shifts are expressed in parts per million (δ scale) downfield from tetramethylsilane and are referenced to the residual signals of CDCl_3 ($\delta = 7.260$ and 77.03 ppm, respectively). Data are presented as follows ^1H NMR: chemical shift, multiplicity (s = singlet, d = doublet, t = triplet, m = multiplet and/or multiple resonances, b = broad), coupling constants, J , in hertz (Hz), integration ^{13}C NMR: chemical shift and type of carbon (CH_3 , CH_2 , CH or C). The type of carbon was assigned by DEPT-135 spectra. FTIR spectra were obtained from neat samples using the attenuated total reflection (ATR) technique. High-resolution mass spectrometry (HRMS) was performed using the EI technique. Optical rotations in chloroform solution (dye concentration, c , expressed in $\text{g}/100\text{ mL}$, *ca.* $0.1 \cdot 10^{-3}$, unless otherwise indicated) were recorded at 293 K on an Anton Paar MCP 100 polarimeter. Fluorescent signatures were recorded using diluted dye solutions (*ca.* $2 \cdot 10^{-6}\text{ M}$) prepared from a concentrated stock solution in acetone (*ca.* 10^{-3} M), after vacuum evaporation of the solvent from a certain amount of sample, and ulterior dilution with the desired solvent of spectroscopic grade. UV-vis absorption and fluorescence spectra were recorded on a Varian (model CARY 4E) spectrophotometer and an Edinburgh Instrument spectrofluorimeter (model FLSP 920), respectively. Fluorescence quantum yields (Φ) were determined from corrected spectra (detector sensibility to the wavelength) by the optically dilute relative method and by the use of the following equation (Eq. 1), where I_{exc} is the luminescent intensity at the excitation wavelength, A_{exc} is the absorbance at the excitation wavelength, $\int I d\lambda$ is the numerically integrated intensity from the luminescence spectra, and n is the index of refraction of the solution. The subscripts R and S denote reference and sample, respectively. PM567 in ethanol ($\Phi^r = 0.84$),¹ and zinc

phtalocyanine in toluene with 1% of pyridine ($\Phi^r = 0.30$),² were used as the reference for **1a-1d** and **2a-2b**, respectively.

$$\Phi_S / \Phi_R = \left(\int I_S d\lambda / \int I_R d\lambda \right) (I_{R,exc} / I_{S,exc}) (A_{R,exc} / A_{S,exc}) (n_S / n_R)^2 \quad \text{Eq. 1}$$

The aforementioned spectrofluorimeter is also equipped with a wavelength-tunable pulsed Fianium laser. Thus, the Time Correlated Single-Photon Counting (TCSPC) technique was used to record the fluorescence decay curves. Fluorescence emission was monitored at the maximum emission wavelength after excitation by the said Fianium at the maximum absorption wavelength. The fluorescence lifetime (τ) was obtained from the slope of the exponential fit of the decay curve, after the deconvolution of the instrumental response signal (recorded by means of a Ludox scattering suspension) by means of an iterative method. The goodness of the exponential fit was controlled by statistical parameters (chi-square, Durbin-Watson and the analysis of the residuals). ECD spectra were recorded on a Jasco (model J-715) spectropolarimeter using standard quartz cells of 1-cm optical-path length in chloroform solution, unless otherwise indicated, at a dye concentration of ca. $3.5 \cdot 10^{-6}$ M. Circularly polarized luminescence (CPL) and total luminescence spectra were recorded at 295 K in degassed chloroform solution (nitrogen was bubbled into the solution), unless otherwise indicated, at a dye concentration of ca. $1.5 \cdot 10^{-3}$ M, on an instrument described previously,³ operating in a differential photon-counting mode. The light source for excitation was a continuous wave 1000 W xenon arc lamp from a Spex Fluorolog-2 spectrofluorimeter, equipped with excitation and emission monochromators with dispersion of 4 nm/mm (SPEX, 1681B). The excitation energy was selected by excitation-fluorescence spectroscopy. To prevent artefacts associated with the presence of linear polarization in the emission,⁴ a high quality linear polarizer was placed in the sample compartment, and aligned so that the excitation beam was linearly polarized in the direction of emission detection (z-axis). The key feature of this geometry is that it ensures that the molecules that have been excited and that are subsequently emitting are isotropically distributed in the plane (x,y) perpendicular to the direction of emission detection. The optical system detection consisted of a focusing lens, long pass filter, and 0.22 m monochromator. The emitted light was detected by a cooled EMI-9558B photomultiplier tube operating in photo-counting mode. The polynomial fit tool implemented in OriginPro 9 was used to fit CPL data points to the corresponding continuous-curve CPL spectrum (4th. order polynomials were used).

2. Synthetic procedures and characterization data

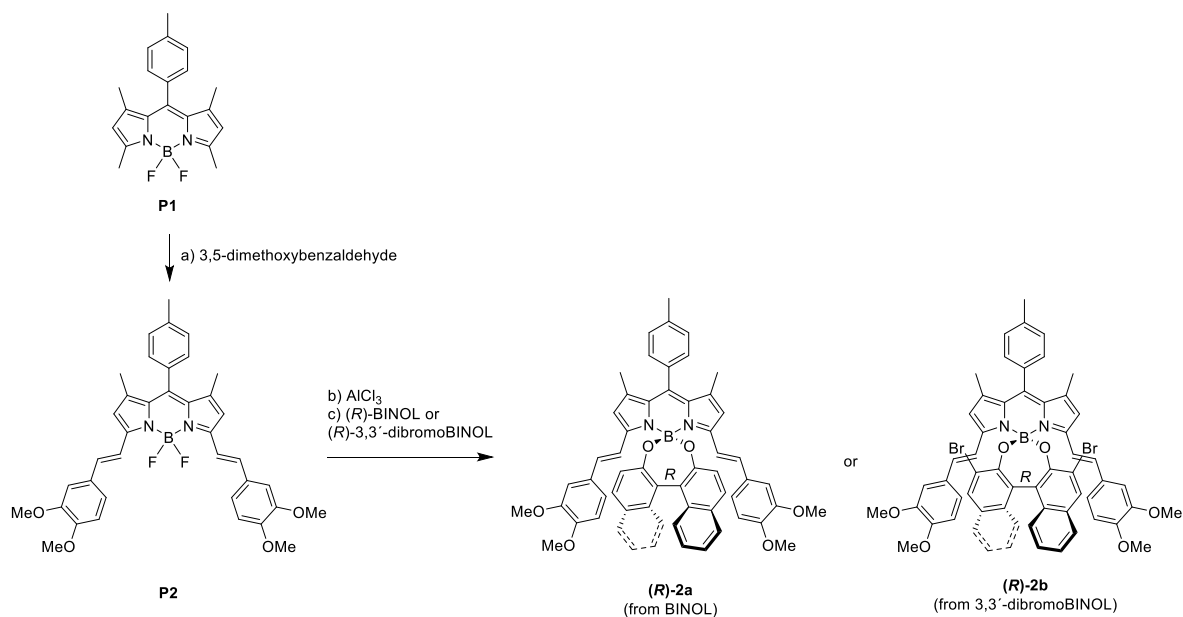


Figure S1. Synthesis of BODIPYs *(R)*-2a and *(R)*-2b.

3,5-Bis[(*E*)-2-(3,4-dimethoxyphenyl)vinyl]-1,7-dimethyl-8-(4-methylphenyl)BODIPY

(P2). A mixture of 1,3,5,7-tetramethyl-8-(4-methylphenyl)BODIPY (**P1**;⁵ 50 mg, 0.15 mmol), 3,4-dimethoxybenzaldehyde (74 mg, 0.44 mmol), acetic acid (44 mg, 0.74 mmol) and piperidine (63 mg, 0.74 mmol) in dry *N,N*-dimethylformamide (1 mL) was submitted to microwave irradiation for 40 min at 120 °C. Then, the resulting mixture was diluted with ethyl acetate (20 mL), washed with water (5x20 mL) and dried over anhydrous Na_2SO_4 . After filtration and solvent evaporation under reduced pressure, the obtained residue was submitted to flash chromatography (silica gel; hexane/ethyl acetate 1:1) to obtain **P2** (54 mg, 57%) as a black solid. R_f 0.36 (silica gel; hexane/ethyl acetate 1:1). ^1H NMR (CDCl_3 , 300 MHz) δ 7.59 (d, $J = 16.2$ Hz, 2H), 7.29 (d, $J = 7.9$ Hz, 2H), 7.23-7.11 (m, 8H), 6.88 (d, $J = 8.3$ Hz, 2H), 6.61 (s, 2H), 3.97 (s, 6H), 3.92 (s, 6H), 2.45 (s, 3H), 1.46 (s, 6H) ppm. ^{13}C NMR (CDCl_3 , 75 MHz) δ 152.6 (C), 150.2 (C), 149.2 (C), 142.0 (C), 138.9 (C), 138.8 (C), 136.1, 133.5 (C), 132.3 (C), 130.0 (C), 129.8 (CH), 128.4 (CH), 121.6 (CH), 117.6 (CH), 117.6 (CH), 111.2 (CH), 109.7 (CH), 56.1 (CH_3), 21.6 (CH_3), 14.9 (CH_3) ppm. FTIR ν 1489, 1268, 1199, 1163 cm^{-1} . HRMS m/z (%): 634.2812 (calcd for: $\text{C}_{38}\text{H}_{37}\text{BF}_2\text{N}_2\text{O}_4$ 634.2814).

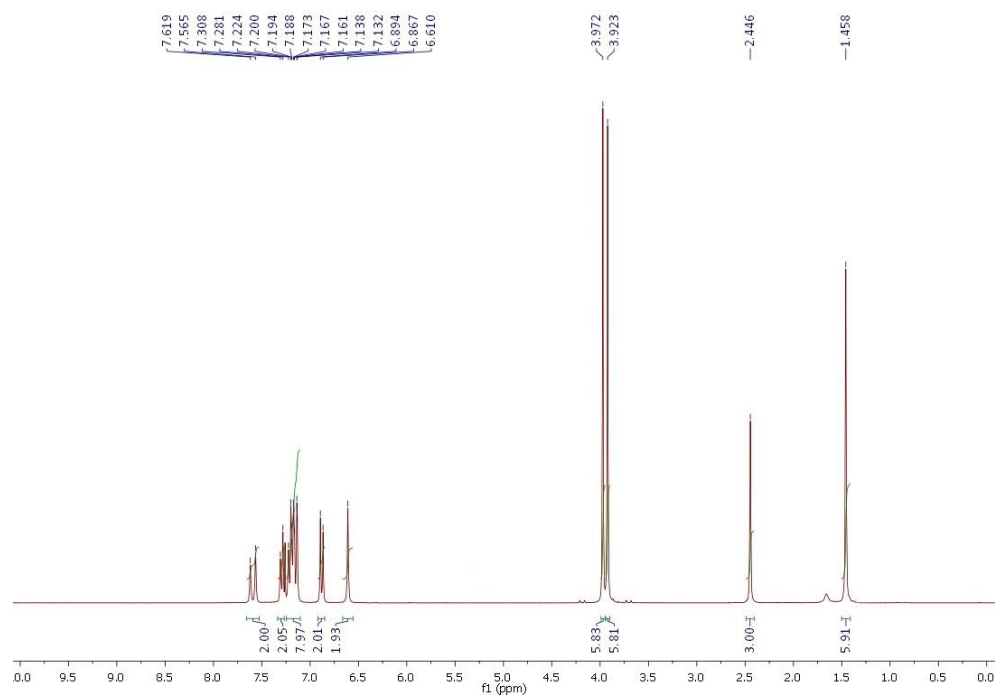
BODIPY (R)-2a. A mixture of **P2** (20 mg, 0.03 mmol) and aluminum chloride (10 mg, 0.08 mmol) in dry CH₂Cl₂ (5 mL) was refluxed under argon atmosphere until reaction completion (reaction monitoring by TLC). The mixture was cooled down to room temperature and, then, a solution of (*R*)-1,1'-bi-2-naphthol ((*R*)-BINOL) (18 mg, 0.06 mmol) in dry acetonitrile (1 mL) was added dropwise. The resulting mixture was stirred at r.t. for additional 18 h, the solvent removed by distillation under reduced pressure, and the resulting residue submitted to flash chromatography (silica gel, hexane/ethyl acetate 7:3) to afford (*R*)-**2a** (13 mg, 47%) as a black solid. $[\alpha]_D^{20} +11192$ (*c* 4.5·10⁻⁴, CHCl₃). ¹H NMR (CDCl₃, 700 MHz) δ 7.61 (d, *J* = 8.1 Hz, 2H), 7.58 (d, *J* = 8.7 Hz, 2H), 7.32 (d, *J* = 7.6 Hz, 2H), 7.28 (d, *J* = 7.7 Hz, 2H), 7.10 (d, *J* = 8.5 Hz, 2H), 7.09 (dd, *J* = 8.1, 6.7 Hz, 2H), 7.07 (d, *J* = 8.6 Hz, 2H), 7.01 (d, *J* = 16.1 Hz, 2H), 6.77 (dd, *J* = 8.6, 6.4 Hz, 2H), 6.51 (d, *J* = 16.1 Hz, 2H), 6.39 (s, 2H), 6.30 (br s, 2H), 6.22 (d, *J* = 8.3 Hz, 2H), 5.92 (d, *J* = 8.3 Hz, 2H), 3.80 (s, 6H), 3.43 (s, 6H), 2.47 (s, 3H), 1.47 (s, 6H) ppm. ¹³C NMR (CDCl₃, 176 MHz) δ 154.4 (C), 154.0 (C), 149.2 (C), 148.3 (C), 141.6 (C), 138.8 (C), 134.4 (C), 133.8 (CH), 133.7 (C), 132.8 (C), 130.3 (C), 129.8 (CH), 129.6 (C), 129.5 (CH), 128.8 (CH), 127.8 (CH), 127.7 (CH), 124.5 (CH), 124.1 (CH), 123.3 (CH), 121.8 (C), 120.1 (CH), 118.8 (CH), 118.5 (CH), 110.8 (CH), 109.8 (CH), 55.9 (CH₃), 55.5 (CH₃), 21.6 (C H₃), 15.1 (CH₃) ppm. FTIR ν 1596, 1545, 1511, 1492, 1267, 1161, 1022 cm⁻¹. HRMS *m/z* 880.3688 (calcd for C₅₈H₄₉BN₂O₆: 880.3684).

BODIPY (R)-2b. A mixture of **P2** (20 mg, 0.03 mmol) and aluminum chloride (10 mg, 0.08 mmol) in dry CH₂Cl₂ (5 mL) was refluxed under argon atmosphere until reaction completion (reaction monitoring by TLC). The mixture was cooled down to room temperature and, then, a solution of (*R*)-3,3'-dibromo-1,1'-bi-2-naphthol ((*R*)-dibromoBINOL; 28 mg, 0.06 mmol) in dry acetonitrile (2 mL) was added dropwise. The resulting mixture was washed with water (2x10 mL) and dried over anhydrous Na₂SO₄. After filtration and solvent evaporation under reduced pressure, the obtained residue was submitted to flash chromatography (silica gel, hexane/ethyl acetate 7:3) to afford (*R*)-**2b** (30 mg, 94%) as a black solid. $[\alpha]_D^{20} +14333$ (*c* 7.5·10⁻⁴, CHCl₃). ¹H NMR (CDCl₃, 300 MHz) δ 7.89 (s, 2H), 7.45 (d, *J* = 8.1 Hz, 2H), 7.33 (d, *J* = 7.9 Hz, 2H), 7.28 (d, *J* = 7.9 Hz, 2H), 7.08 (ddd, *J* = 8.1, 6.8, 1.2 Hz, 2H), 6.89 (d, *J* = 8.7 Hz, 2H), 6.85 (d, *J* = 16.0 Hz, 2H), 6.76 (ddd, *J* = 8.5, 6.9, 1.3 Hz, 2H), 6.55 (d, *J* = 16.0 Hz, 2H), 6.40 (s, 2H), 6.30 (d, *J* = 8.4 Hz, 2H), 6.24 (d, *J* = 1.9 Hz, 2H), 6.05 (dd, *J* = 8.4, 1.9 Hz, 2H), 3.82 (s, 6H), 3.44 (s,

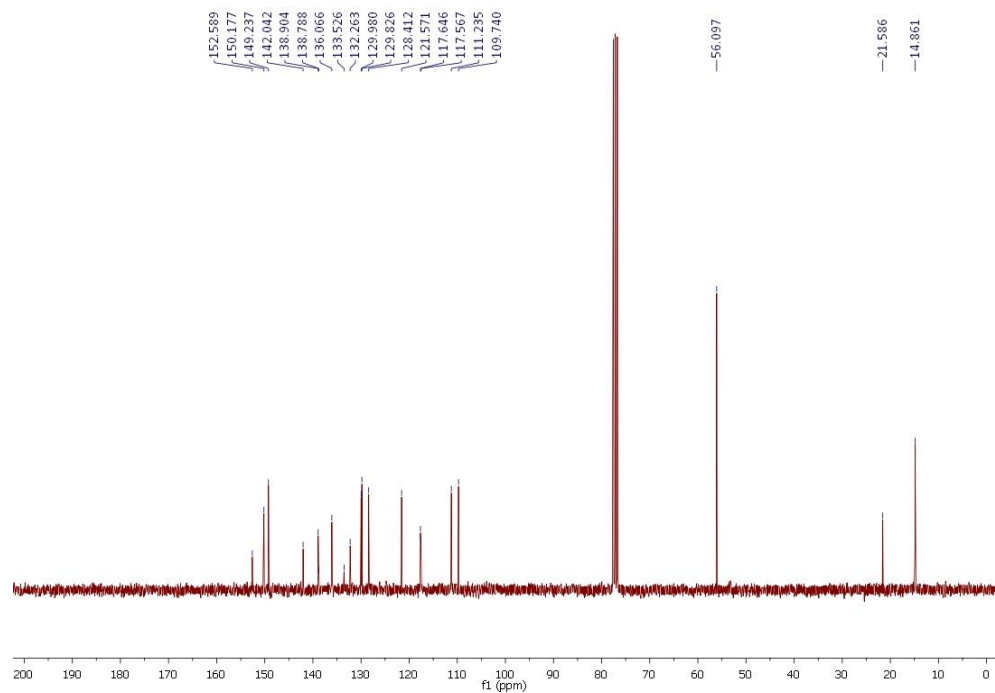
6H), 2.47 (s, 3H), 1.49 (s, 6H) ppm. ^{13}C NMR (CDCl_3 , 75 MHz) δ 154.0 (C), 150.7 (C), 149.2 (C), 148.3 (C), 141.9 (C), 138.9 (C), 138.8 (C), 135.1 (C), 133.8 (CH), 132.8 (C), 132.0 (CH), 130.4 (C), 129.8 (CH), 128.6 (CH), 127.4 (CH), 126.8 (CH), 124.9 (CH), 124.3 (CH), 123.0 (C), 120.1 (CH), 119.5 (C), 119.3 (CH), 118.1 (CH), 110.6 (CH), 109.4 (CH), 55.9 (CH_3), 55.4 (CH_3), 21.6 (CH_3), 15.0 (CH_3) ppm. FTIR ν 3055, 1491, 1268, 1160, 990 cm^{-1} . HRMS m/z 1036.1897 (calcd for $\text{C}_{58}\text{H}_{47}\text{BBr}_2\text{N}_2\text{O}_6$: 1036.1894).

3. ^1H - and ^{13}C -NMR spectra

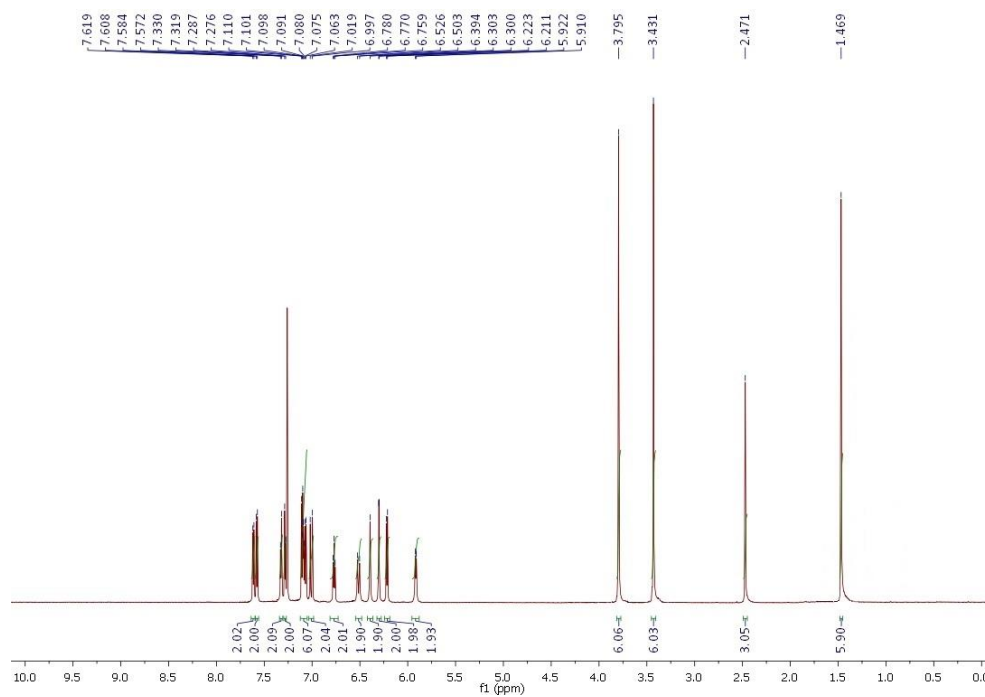
^1H NMR (CDCl_3 , 300 MHz) spectrum of P2.



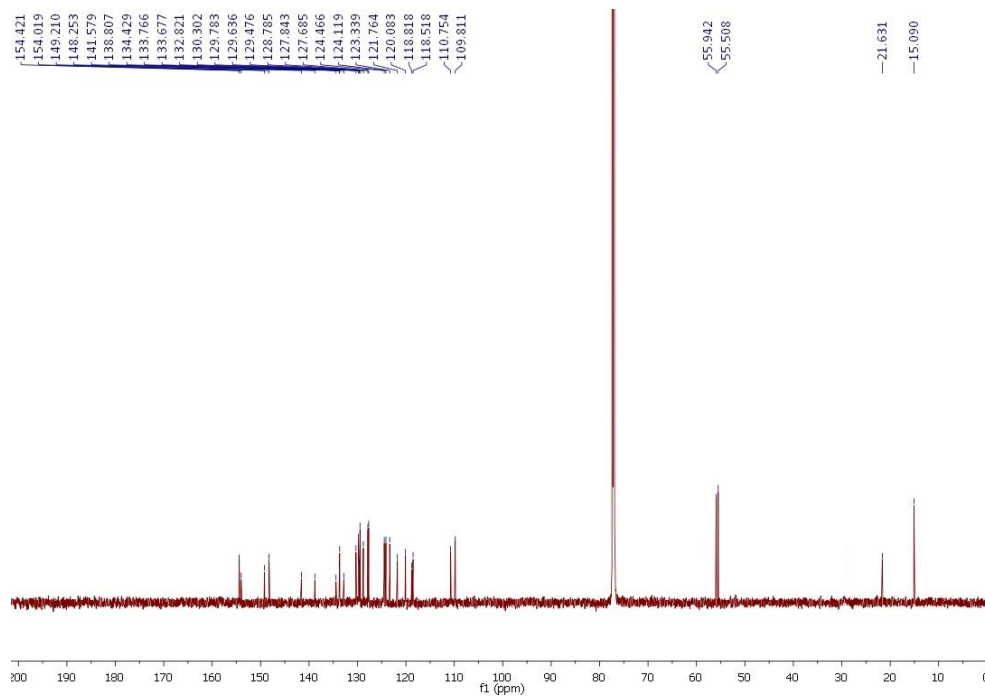
^{13}C NMR (CDCl_3 , 75 MHz) spectrum of P2.



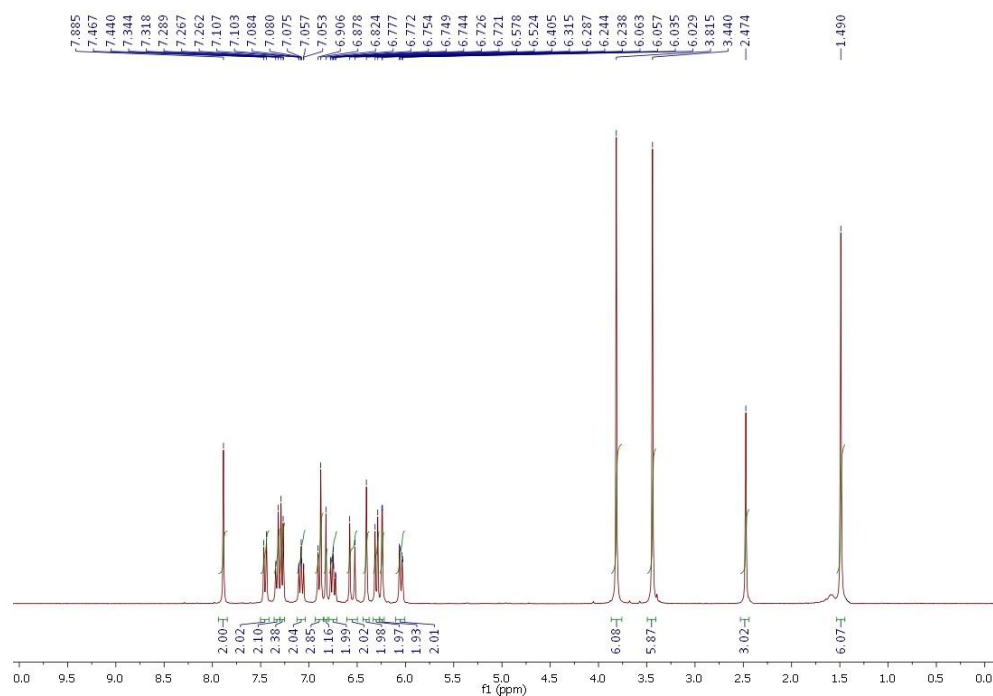
¹H NMR (CDCl₃, 700 MHz) spectrum of (R)-2a.



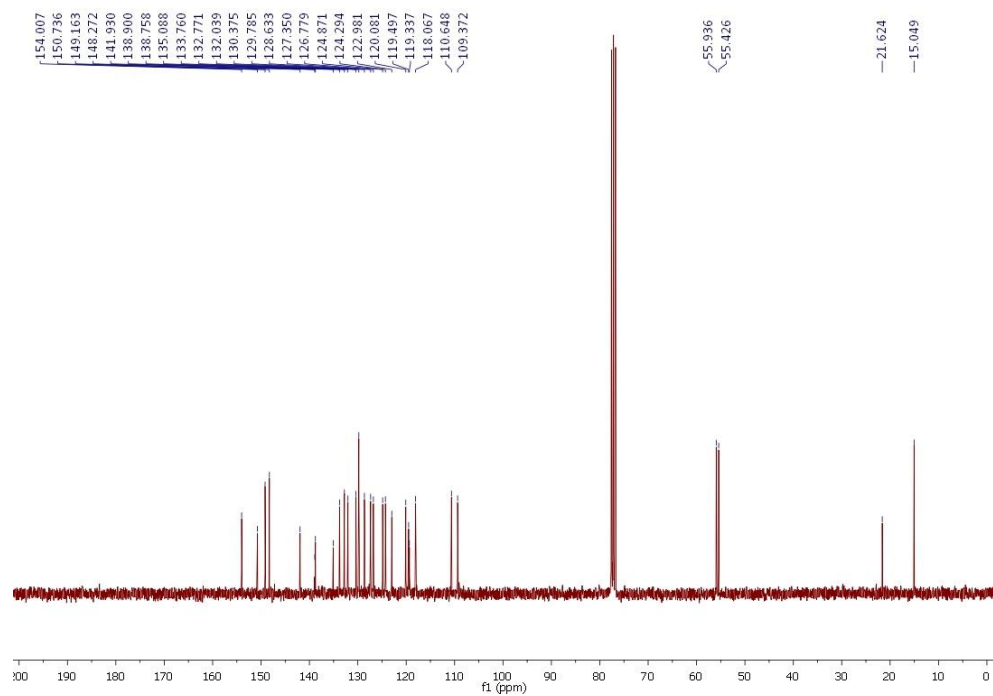
¹³C NMR (CDCl₃, 176 MHz) spectrum of (R)-2a.



¹H NMR (CDCl₃, 300 MHz) spectrum of (R)-2b.



¹³C NMR (CDCl₃, 75 MHz) spectrum of (R)-2b.



4. Photophysical properties

Table S1. Fluorescence and chiroptical signatures of (*R*)-**1a-d** and (*R*)-**2a-b** in chloroform.

O-BODIPY	λ_{ab}^a (nm)	$\epsilon_{max} \cdot 10^{-4}^b$ (M ⁻¹ cm ⁻¹)	λ_{fl}^c (nm)	Φ^d	$[\alpha]_D^{20}^e$	$g_{abs} \cdot 10^3^{f,g}$	$g_{lum} \cdot 10^3^{g,h}$
(<i>R</i>)- 1a ⁱ	525.0	6.0	550.0	0.47	-5076	-0.9 (525)	+0.7 (568)
(<i>R</i>)- 1b ^j	527.0	7.4	547.0	0.69	-4144	-0.9 (528)	-0.6 (589)
(<i>R</i>)- 1c	524.0	7.2	548.0	0.82	-1677	-0.3 (525)	-0.3 (580)
(<i>R</i>)- 1d	530.0	5.9	553.0	0.53	-2601	-0.6 (529)	+0.8 (628)
(<i>R</i>)- 2a	653.5	6.5	675.0	0.66	+11192 ^{k,l}	-1.2 (658)	-0.5 (752) ^m
(<i>R</i>)- 2b	652.0	7.4	678.0	0.69	+14333 ^{n,l}	-1.3 (656)	-0.6 (741)

^aAbsorption wavelength. ^bMolar absorption. ^cFluorescence wavelength. ^dFluorescence quantum yield. ^eOptical rotation. ^fMaximum absorption dissymmetry factor. ^gWavelength (in nm) for the reported g_{abs} and g_{lum} values is dated into parenthesis. ^hMaximum luminescence dissymmetry factor. ⁱData collected from references [6] and [7]. ^jData collected from references [7] and [8]. ^k $c = 4.3 \cdot 10^{-4}$. ^lHuge optical rotation for (*R*)-**2a-b**, when compared to (*R*)-**1a-d**, is associated to anomalous ORD (optical rotatory dispersion) due to light absorption at the used sodium D-line (589 nm). ^mAcetone is used as the solvent instead of chloroform. ⁿ $c = 7.5 \cdot 10^{-4}$.

Table S2. Fluorescence signatures of (*R*)-**2a** and (*R*)-**2b** in different solvents.

O-BODIPY solvent	λ_{ab}^a (nm)	$\epsilon_{max} \cdot 10^{-4}^b$ (M ⁻¹ cm ⁻¹)	λ_{fl}^c (nm)	Φ^d	τ^e (ns)
(<i>R</i>)-2a					
<i>cyclohexane</i>	652.5	6.5	670.0	0.64	3.96
<i>chloroform</i>	653.5	6.6	675.0	0.66	3.91
<i>acetone</i>	650.0	7.0	671.5	0.65	3.96
<i>acetonitrile</i>	648.0	6.6	670.5	0.67	3.75
(<i>R</i>)-2b					
<i>cyclohexane</i>	654.0	7.7	678.0	0.66	3.99
<i>chloroform</i>	652.0	7.4	678.0	0.69	3.94
<i>acetone</i>	655.0	9.1	679.0	0.62	4.06
<i>acetonitrile</i>	652.0	8.5	677.0	0.62	4.07

^aAbsorption wavelength. ^bMolar absorption. ^cFluorescence wavelength. ^dFluorescence quantum yield. ^eFluorescence lifetime.

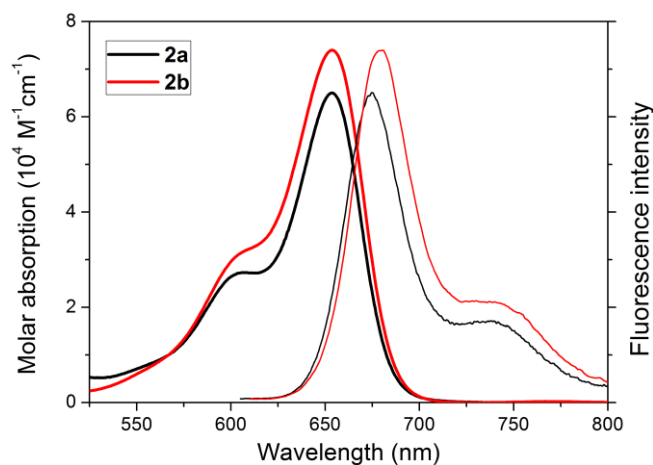


Figure S2. UV-vis absorption (thick line) and normalized fluorescence (thin line) spectra of (*R*)-**2a** and (*R*)-**2b** in diluted chloroform solution.

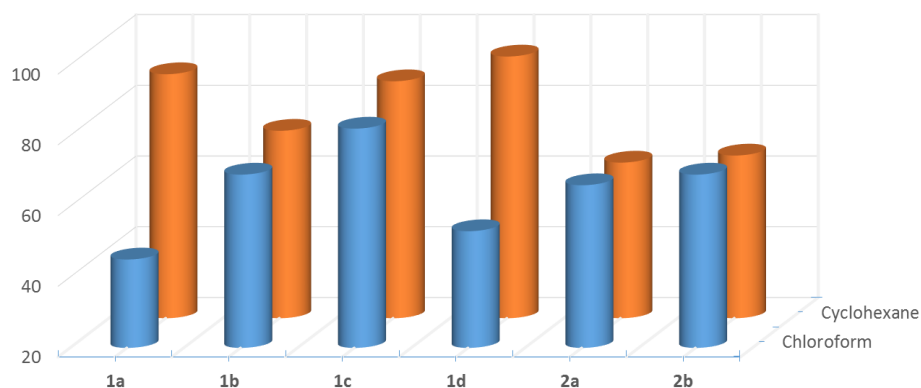


Figure S3. Evolution of the fluorescence quantum yield of **1a-d** (data from reference 7), as well as **2a-b** (data from Table S2) in two solvents of different polarity. Significant loss of the fluorescence efficiency in polar chloroform when compared to that attained in apolar cyclohexane demonstrates ongoing significant ICT, which is only accounted for **1a** and **1d**, but not for **1b**, **1c**, **2a** and **2b**.

References

- [1] F. López Arbeloa, J. Bañuelos, V. Martínez, T. Arbeloa, I López Arbeloa, *Int. Rev. Phys. Chem.* **2005**, *24*, 339-374.
- [2] P. S. Vincent, E. M. Voigt, K. E. Rieckhoff, *J. Chem. Phys.* **1971**, *55*, 4131-4140.
- [3] E. Brunet, L. Jiménez, M. de Victoria-Rodríguez, V: Luu, G. Muller, O. Juanes, J. C. Rodríguez-Ubis, *Microporous Mesoporous Mater.* **2013**, *169*, 222-234, and references cited therein.
- [4] H. P. J. M. Dekkers, P. F. Moraal, J. M. Timper, J. P.; Riehl, *Appl. Spectrosc.* **1985**, *39*, 818-821.
- [5] A. Cui, X. Peng, J. Fan, X. Chen, Y. Wu, B. Guo, *J. Photochem. Photobiol. A: Chem.* **2007**, *186*, 85-92.
- [6] E. M. Sanchez-Carnerero, F. Moreno, B. L. Maroto, A. R. Agarrabeitia, M. J. Ortiz, B. G. Vo, G. Muller, S. de la Moya, *J. Am. Chem. Soc.* **2014**, *136*, 3346-3349.
- [7] L. Gartzia-Rivero, E. M. Sánchez-Carnerero, J. Jiménez, J. Bañuelos, F. Moreno, B. L. Maroto, I. López-Arbeloa, S. de la Moya, *Dalton Trans.* **2017**, *46*, 11830-11839.
- [8] J. Jiménez, L. Cerdán, F. Moreno, B. L. Maroto, I. García-Moreno, J. L. Lunkey, G. Muller, S. de la Moya, *J. Phys. Chem. C* **2017**, *121*, 5287-5292.